



Cite this: *Phys. Chem. Chem. Phys.*,
2017, **19**, 1644

On the accuracy of the general, state-specific polarizable-continuum model for the description of correlated ground- and excited states in solution†

Jan-Michael Mewes,^{*ab} John M. Herbert^c and Andreas Dreuw^a

Equilibrium and non-equilibrium formulations of the state-specific polarizable-continuum model (SS-PCM) are evaluated in combination with correlated ground- and excited-state densities provided by the algebraic-diagrammatic construction method (ADC) for the polarization propagator via the computationally efficient intermediate-state representation (ISR) formalism. Since the influence of the SS-PCM onto quantum-chemical method is naturally limited to the presence of the apparent surface charges in the one-electron Hamiltonian and hence fully contained in the polarized MOs, the herein presented solvent model can be combined with all implemented orders and variants of ADC. Employing ADC/SS-PCM, the symmetric, ionized dimers of neon, ethene and nitromethane are investigated. Their broken-symmetry wavefunctions exhibit a low-lying charge-transfer state that is symmetry-equivalent to the ground state. This curious though ultimately artificial feature is convenient as it allows for a direct comparison of ADC/SS-PCM for the CT state to the Møller–Plesset/PCM description of the ground state. The agreement down to 0.02 eV for a wide range of dielectric constants validates the ADC/SS-PCM approach. Eventually, the relaxed potential-energy surfaces of the ground and lowest excited states of 4-(*N,N*)-dimethylaminobenzonitrile in cyclohexane and acetonitrile are computed, and it is demonstrated that the ADC(2)/SS-PCM approach affords excellent agreement with experimental fluorescence data. Only at the ADC(3) level of theory, however, the experimentally observed solvent-dependent dual fluorescence can be explained.

Received 30th August 2016,
Accepted 28th November 2016

DOI: 10.1039/c6cp05986d

www.rsc.org/pccp

1 Introduction

The approximate modeling of molecular environments for quantum-chemical calculations is a very active field of research.^{1–8} Polarizable continuum models¹ (PCMs) offer an efficient way to incorporate bulk electrostatic effects, typically the dominant solvation effect for small, polar molecules and in particular for charge-transfer states. While PCMs are certainly not the most accurate or elaborate representation of a molecular environment, a key advantage is their straightforward application. Once the construction of a molecular cavity for the solute is specified, PCMs are essentially “black box” computational models with

only two parameters: the macroscopic dielectric constant ϵ and its analog in the range of optical frequencies, the optical dielectric constant $\epsilon_{\text{opt}} = n^2$, where n denotes the solvent's index of refraction. Despite their simplicity, PCMs usually provide a reasonable estimate of the influence of the environment in a single calculation, if explicit interactions like *e.g.* hydrogen-bonds are weak or absent.⁹ In combination with correlated *ab initio* methods for the QM part of the calculation, this particularly applies to the practically important class of charge-transfer states, as nicely demonstrated in ref. 10 and 11. Computational efficiency and straightforward setup of continuum models are largely due to the fact that they circumvent the need for sampling of the environment, which is included implicitly in the macroscopic parameters.

Here, we report the implementation of a self-consistent PCM description of the environment following the well-established state-specific (SS) approach^{12–19} for long-lived, solvent-equilibrated excited-states. Correlated ground- and excited-state wavefunctions and densities are obtained with the algebraic-diagrammatic construction method for the polarization propagator (ADC) and the intermediate-state representation (ISR) formalism.²⁰ For its

^a Interdisciplinary Center for Scientific Computing, Rupprechts-Karls University, Im Neuenheimer Feld 205, 69120 Heidelberg, Germany.
E-mail: janmewes@janmewes.de

^b Centre for Theoretical Chemistry and Physics, The New Zealand Institute for Advanced Study (NZIAS), Massey University Albany, Private Bag 102904, Auckland 0745, New Zealand

^c Department of Chemistry and Biochemistry, The Ohio State University, Columbus, OH 43210, USA

† Electronic supplementary information (ESI) available. See DOI: 10.1039/c6cp05986d

evaluation, this new approach is combined with the recently presented perturbative, state-specific (ptSS) non-equilibrium corrections for vertical transitions,^{9,21} which enables a numerically efficient investigation of processes like fluorescence, phosphorescence and excited-state absorption at up to third order of ADC, ADC(3). This high level of electronic-structure theory can be necessary to arrive at a balanced description of excited states of different character, as will be shown and discussed for the example of dimethylamino-benzonitrile (DMABN) in Section 4.2.

Self-consistent implementations of the SS-PCM approach for long-lived excited states, *i.e.*, equilibrium solvation have been presented in combination with time-dependent DFT,²² EOM-CCSD^{23–25} and for the PCM-related COSMO²⁶ also with ADC(2) (ADC/COSMO).²⁷ For the latter, Lunkenheimer *et al.* self-consistently include transition-density related linear-response (LR) contributions into the ADC(2) equations in addition to the charge-density contributions of the SS-PCM formalism. The LR-PCM formalism,^{28,29} which has so far been regarded as an alternative to the SS formalism, has in the past been used to obtain non-equilibrium corrections as well as to describe solvent-relaxed states.^{30,31} In contrast to the SS-PCM formalism, however, the physical interpretation of the LR formalism is subject of ongoing debate,^{9,27,32} and direct comparison of the LR- and SS-PCM formalism suggests that the latter affords more accurate solvent-relaxed geometries and emission spectra.³³ In the context of non-equilibrium corrections to ADC(2) and ADC(3) excitation energies, we obtain more accurate solvatochromatic shifts using the SS-PCM formalism as compared to the LR-PCM approach or a combination of the latter two.⁹

Hence, unlike ADC/COSMO, the herein presented ADC/SS-PCM strictly follows the SS approach. Contributions from the solvent are included only at the level of the one-electron Hamiltonian and thus fully contained in the respective, polarized MOs. This provides the advantage that the ADC equations can remain unchanged and the SS-PCM approach can be applied in identical fashion to any order and variant of ADC or related excited-state method. So far, we have tested the approach in combination with core-valence separated (CVS)ADC,^{34,35} spin-opposite scaled (SOS)ADC,³⁶ and spin-flip (SF)ADC³⁷ (results not shown in this work). In particular for SF-ADC, the herein presented self-consistent equilibrium solvation approach constitutes a valuable tool to investigate molecules with a complicated electronic structure in solution, as it allows to relax the solvent with respect to any state (*e.g.* the physical ground state) and not just the high-spin reference. Ultimately, the resulting solvent-equilibrated wavefunctions can be investigated using the visualization and analysis tools provided by libwfa.³⁸ Another difference to the ADC/COSMO approach concerns the excited-state densities. While ADC/COSMO employs relaxed densities, the excited-state densities used in our ADC/SS-PCM approach are obtained *via* the intermediate-state representation (ISR) formalism as elaborated in ref. 9. This circumvents the need to compute any orbital response, such that the solvent model adds only negligible overhead to the cost of a gas-phase ADC calculation.

To demonstrate that this combination of ADC with the SS-PCM provides physically meaningful results, we will at first perform tests on a set of symmetric ionized dimers whose symmetry-broken ground state is symmetry-equivalent to the lowest charge-transfer excited state. This completely artificial test system allows the new ADC/SS-PCM approach to be compared and validated against ground-state Møller–Plesset calculations. Eventually, we employ the prominent example of 4-(*N,N*)-dimethylaminobenzonitrile (DMABN) to showcase the performance of ADC/SS-PCM at second and third order of perturbation theory for the prediction of fluorescence and solvent-relaxed state energies in solution.

This paper is structured as follows: Section 2 presents the formalism and implementation. Section 3 describes the technical details of the calculations. In Section 4 we evaluate and discuss the ADC/SS-PCM approach as well as the different approaches to treat electron correlation in the PCM framework, first in symmetric, ionic dimers and second in the prototypical charge-transfer compound, 4-(*N,N*)-dimethylaminobenzonitrile (DMABN). Section 5 summarizes our conclusions.

2 Formalism and implementation

The formalism of the self-consistent ADC/SS-PCM implementation is described here, following the notation in ref. 9 and 21, where the analogous, perturbative, non-equilibrium theory is presented.

2.1 Ground-state equilibrium PCM

In any self-consistent reaction field (SCRf) calculation, the interaction of the ground state with the reaction field provided by the PCM is formally contained in the so-called reaction-field operator, $\hat{R}(0)$:

$$[\hat{H}^{\text{vac}} + \hat{R}(0)]|0\rangle = E_0|0\rangle. \quad (1)$$

In practice, the molecule is placed in a cavity with the surface S divided into discretized surface elements s , which in our implementation are Lebedev grid points situated on atom-centered spheres.³⁹ The operator \hat{R} formally accounts for the interaction of the molecular electrostatic potential (ESP) $V(r)$ with the apparent surface charge (ASC) $\gamma(s)$ of a state $|i\rangle$ according to

$$\hat{R}(i) \equiv \hat{R}_i = \int_S \frac{\gamma_i(s)}{|r-s|} ds = \int_S \hat{V}(r,s) \gamma_i(s) ds, \quad (2)$$

where $\hat{V}(r,s) = |r-s|^{-1}$. The operator $\hat{R}(i)$ can be further simplified by carrying out the integration over r , to yield

$$\begin{aligned} \langle 0|\hat{R}_i|0\rangle &= \int_S \langle 0|\hat{V}(r,s)|0\rangle \gamma_i(s) ds \\ &= \int_S V_0(s) \gamma_i(s) ds = E_{0-i}, \end{aligned} \quad (3)$$

where $V_0(s)$ is the ESP for state $|0\rangle$, evaluated at position s . In practice, the ASC for state i , $\gamma_i(s)$, is represented by a set of Gaussian-blurred point charges at the positions of the surface elements s .³⁹

The quantity E_{0-i} that results from integration over the cavity surface in eqn (3) is the total solute–solvent interaction energy for state $|0\rangle$ (the initial state), where the polarization is induced by state $|i\rangle$. If solute and solvent are in equilibrium, as in the ground state or a long-lived excited state, then $|0\rangle$ and $|i\rangle$ should represent the same state.

The ASC is generated by the solvent-response operator

$$\hat{Q} = \int_S \hat{V}(r, s') A_e^{-1}(s, s') ds', \quad (4)$$

such that the ASC for state i is

$$\gamma_i(s) = \langle i | \hat{Q} | i \rangle = \int_S V_i(s') A_e^{-1}(s, s') ds'. \quad (5)$$

These equations depend on the PCM kernel A_e^{-1} , which depends on the cavity geometry as well as the dielectric constant, and is what discriminates between various flavors of PCM, *e.g.*, the conductor-like approximation (C-PCM),³⁰ the integral-equation formalism (IEF-PCM),⁴⁰ or the surface and simulated volume polarization for electrostatics [SS(V)PE] approach.^{41,42}

2.2 Free energy

Because the concept of a dielectric constant implicitly includes solvent averaging, the electrostatic energies in PCM theory are free energies, whereas up to this point we have introduced expressions for interaction energies only. To obtain free energies, one must account for the work associated with polarizing the continuum, which amounts to half of the electrostatic interaction energy.^{43,44} Thus, the free energy of an equilibrated state $|i\rangle$ is

$$G^{\text{solv}} = \langle i | \hat{H}^{\text{vac}} + \frac{1}{2} \hat{R}_i | i \rangle. \quad (6)$$

For the case of state $|i\rangle$ in the frozen reaction field of an equilibrated reference state $|\text{eq}\rangle$, one has to keep in mind that the polarization work is incurred in the equilibrated reference state and thus

$$G_i^{\text{Eq}(\text{eq})} = \langle i | \hat{H}^{\text{vac}} + \hat{R}_{\text{eq}} | i \rangle - \frac{1}{2} \langle \text{eq} | \hat{R}_{\text{eq}} | \text{eq} \rangle. \quad (7)$$

2.3 Equilibration of the excited-state wave function

Any post-Hartree–Fock calculation performed using the polarized MOs afforded by an SCRf calculation implicitly includes the interaction with the solvent field. As such, calculation of an equilibrated excited-state wave function using ADC requires that the SCF calculation is carried out in the presence of an excited-state reaction field, which of course is not known in advance. An iterative procedure is therefore required during which the reaction-field operator $\hat{R}(t)$ and corresponding wave function $|i\rangle$ achieve self-consistency. Typically (but not necessarily), the starting point for these iterations is the excited-state density (or the respective electrostatic potential or reaction field) computed in a ground-state relaxed solvent field (or in the gas-phase). In the next step, the SCF is iterated to convergence in the presence of the reaction field of the excited-state wavefunction $|i\rangle$, and another excited-state calculation is performed using the new MOs, in order to update $|i\rangle$; convergence to *ca.* 1 meV is typically

achieved in about five iterations and to 1 meV in about seven (see ESI†). The same procedure can be used to equilibrate the reaction field of the ground state using a correlated density, which corresponds to the perturbation-energy-and-density approach of ref. 45 (see below).

2.4 From eigenvalues to physical energies

The combination of the two iterative procedures, namely, an MP/ADC calculation with the ground-state reference as inner loop and the solvent-field iterations with a different excited-state reference as an outer loop, leads to complications in the assignment of energies to physical states and processes, which we elaborate here. In the context of the quantum-chemical calculation (inner loop), the energy of the ground state is the MP energy obtained in the frozen reaction field of the equilibrated (outer loop) reference state, and the excited-state energies are the sum of this ground-state energy plus an ADC excitation energy. Thus far, the polarization term in the form $\frac{1}{2} \langle \text{eq} | \hat{R}_{\text{eq}} | \text{eq} \rangle$ has been included explicitly at the SCF level of the calculation, whereas the interaction with the ASC of the reference state, *i.e.*, $\langle i | \hat{R}_{\text{eq}} | i \rangle$ is included implicitly *via* the MOs. Accordingly, the excitation and total energies resulting from an ADC calculation employing polarized MOs correspond to the energies of the respective states in the frozen reaction field of the equilibrated (outer-loop reference) state. Hence, apart from the energy of the latter, the energies of the other (excited and ground) states have no immediate physical relevance during this stage of the calculation.

Only in the context of the solvent-field iterations (outer loop) do the energies of the out-of-equilibrium states acquire physical significance. For this purpose, they must be regarded in the non-equilibrium limit according to the Franck–Condon principle, with only the slow component \hat{R}^s of the solvent polarization frozen with respect to the equilibrated state, whereas the fast component \hat{R}^f is relaxed. To take this into account, we have modified the ptSS to allow for an arbitrary reference state that need not be the ground state. For this purpose, all ground-state quantities in eqn (16) of ref. 9 are replaced with those of the equilibrated reference state $|\text{eq}\rangle$, yielding

$$G_i^{\text{ptSS}} = \langle i^{(0)} | \hat{R}_i^f | i^{(0)} \rangle - \langle i^{(0)} | \hat{R}_{\text{eq}}^f | i^{(0)} \rangle - \frac{1}{2} \left(\langle i^{(0)} | \hat{R}_i^f | i^{(0)} \rangle - \langle \text{eq} | \hat{R}_{\text{eq}}^f | \text{eq} \rangle \right) + \frac{1}{2} \int_S \left(\gamma_i^f(s) - \gamma_{\text{eq}}^f(s) \right) V_{\gamma_{\text{eq}}^f}(s) ds. \quad (8)$$

Here, $i^{(0)}$ refers to the zeroth-order wave function of the state of interest, $|i\rangle$, in the non-equilibrium limit. The first line of eqn (8) accounts for the change in the solute–solvent interaction energy, the second line accounts for the change in polarization, and the third line is the change in the self-interaction between the fast and slow surface charges.

As soon as the reaction field is converged, the sum of the MP ground-state energy, the ADC excitation energy and the respective ptSS correction corresponds to the energy of the state $|i\rangle$ in the non-equilibrium limit, but only with respect to a vertical

transition from the reference state, *e.g.* via fluorescence, phosphorescence or excited-state absorption. Note that while the transition probability for fluorescence from the reference to the ground state is computed per default, state-to-state transition properties (*e.g.* for excited-state absorption) are also available but have to be requested explicitly.

To clearly discriminate between these “theoretical” and “physical” quantities, we will embrace the following partition: Total and transition energies which are direct results of the respective HF/MP/ADC calculations for the ground and excited states are denoted PCM zeroth order. They correspond to the energy eigenvalues of the respective wave functions in the frozen ASC of the equilibrated state and hence do not include perturbative, non-equilibrium corrections. Excited states are sorted with respect to these energies. Transition and total energies including ptSS non-equilibrium corrections are denoted PCM first order. The respective ptSS non-equilibrium corrections are always computed with respect to the equilibrated reference state.

2.5 Electron correlation in the PCM framework

To obtain meaningful results from the comparison of the total energies of the ionized dimers computed with ADC(2)/SS-PCM on the one hand and MP/PCM on the other, it is important to treat the influence of electron correlation onto the solute–solvent interaction on an equal footing. For the MP ground-state, several distinct ways have been suggested and explored,^{46–48} which we discuss in the following:

(1) PerTurbation-Energy (PTE) approach: Use the solute–solvent interaction energy computed self-consistently from the SCF density, then use the resulting, polarized Hartree-Fock (HF) orbitals for the post-HF calculation, which is MP2 in the present work.

(2a) PerTurbation-Density (PTD) approach: Compute HF orbitals and correlation energy in the gas-phase, then obtain the solute–solvent interaction energy from a PCM calculation with the correlated gas-phase density.

(3) PerTurbation-Energy-and-Density (PTED, also PTDE) approach: Equilibrate the correlated density and the solvent field such that the solute–solvent interaction is self-consistently included in the MP2 total energy.

A schematic representation of these various methods is presented in Fig. 1. At first glance, the self-consistent PTED scheme appears to offer the most sophisticated treatment of the influence of electron correlation onto the solute–solvent interaction, which moreover closely resembles the ADC(2)/SS-PCM approach. In the case of MP2, however, Ángyán⁴⁵ demonstrated that this iterative scheme involves terms that are at least fourth order in the density and therefore inconsistent with the respective level of perturbation theory. The numerical examples in ref. 46–48 show that the PTE and PTED schemes yield nearly identical total energies, although this might have been the result of small system sizes and basis sets. To further explore this issue, we include the total energies and properties computed with both, the PTE and PTED approaches into our comparison (Section 4.1), which does not only involve larger systems, but also the

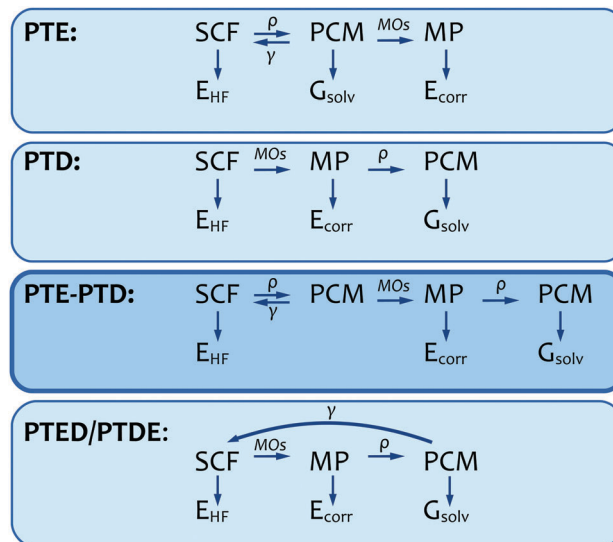


Fig. 1 Flowchart of the different approaches to include electron correlation in a PCM framework. Here, ρ refers to the charge density and γ to the apparent surface charge. The down-pointing arrows indicate at which point in the procedure the HF, solvation and correlation energies are computed. Only in the iterative PTED scheme are the MP density and the solvent field iterated to self-consistency and therefore correlation contributions to the solute–solvent interaction are contained in the MOs. In all other schemes, the MOs contain the interaction with the solvent field, computed for the SCF density. The solvent field equilibration for an excited state is essentially identical to a PTED calculation, but with an ADC instead of an MP density.

nitromethane molecule, whose electrostatic nature is strongly affected by correlation effects.

Our experience with the ptSS approach for ADC excited states⁹ suggests that it is desirable to compute at least the solvent field for a correlated density, due to the fact that excitation energies contain the interaction with the nuclear component of the ground-state solvent field in zeroth order. Following this insight, we developed a correction related to the PTD scheme that eliminates systematic errors due to the neglect of correlation effects and improves the accuracy of the ptSS approach for excitation energies. In ref. 9 we called this the “PTD” approach, but to distinguish this from the PTD method for the ground state described above, we refer to it here as:

(2b) PTE-PTD approach: Combination of PTD and PTE in which polarized HF orbitals from a PTE calculation are used for the PTD post-HF procedure. Obtain the final solute–solvent interaction energy and solvent field for the correlated (ground and/or excited state) density from an additional PCM calculation with the MP density. Although initially developed as a correction to excitation energies,⁹ this may also be used to correct the MP ground-state energy.

Within the PTE-PTD scheme, which we also investigate in Section 4.1, the interaction energy of any state’s density with the HF and MP solvent reaction fields is computed explicitly from stored densities and electrostatic potentials, after the calculation has converged. For this purpose, the (unrelaxed) MP density computed from the polarized HF orbitals is used. Eventually the interaction with the HF solvent field, which is implicitly

contained in the energies as elaborated in Section 2.3, is calculated explicitly and can be replaced with the respective quantity computed for the MP density.

3 Computational details

3.1 Software

All ADC/SS-PCM calculations were carried out using a locally-modified version of Q-Chem⁴⁹ v. 4.3.2 and unless stated otherwise employ Dunning's correlation-consistent double- and triple- ζ basis sets.⁵⁰ The PCM implemented in Q-Chem was used with default settings, *i.e.*, a smooth Lebedev-grid based cavity construction³⁹ with Bondi's atomic van der Waals radii,^{51,52} scaled by a factor of 1.2. Our recently-introduced ptSS non-equilibrium solvent correction⁹ was used to obtain a perturbative estimate of the relaxed energies (using the full dielectric constant in place of ϵ_{opt}) as well as in the originally intended purpose, *i.e.*, to compute non-equilibrium corrections to state energies in solution. The ground-state geometry of DMABN was computed at the RI-MP2/cc-pVDZ level using Orca v. 3.0.1.⁵³ Excited-state geometries of DMABN were computed at the RI-ADC(2)/cc-pVDZ level using Turbomole v. 6.3.1.⁵⁴

3.2 Broken-symmetry wave functions for ionic dimers

Calculations on the symmetric ionic dimers (separation 1 nm) were performed without point-group symmetry, and the SCF solution was converged to an asymmetrically-charged, broken-symmetry solution. The resulting (physically incorrect) wave function exhibits an energetically low-lying charge-transfer state, which is a formally symmetric "charge inverse" to the ground state, *e.g.*,



A method that perfectly describes orbital relaxation upon charge transfer excitation would afford an excitation energy of zero for the formally-identical charge-transfer (FICT) state in eqn (9). In practice, however, the MOs are optimized for the asymmetrically-charged ground state and approximate single-reference excited-state methods cannot provide quantitative orbital relaxation, so the gas-phase excitation energies $\Omega_{\text{vac}}^{\text{FICT}}$ for the FICT state differ significantly from zero. For the methods and systems considered in this work, $\Omega_{\text{vac}}^{\text{FICT}}$ ranges from -1 eV to $+1$ eV. However, this constant difference does not present a problem in the context of this work. It is computed in the gas phase and subtracted from the energy differences obtained from PCM calculations to obtain the energy difference shown in the plots:

$$\Delta E_{\text{plot}} = E_{\text{ADC/SS-PCM}}^{\text{FICT}} - E_{\text{MP/PCM}}^{\text{gs}} - \Omega_{\text{vac}}^{\text{FICT}} \quad (10)$$

4 Results and discussion

4.1 Symmetric ionic dimers

As a first test of the internal consistency of the ADC/SS-PCM approach and to shed some light onto the different approaches to treat electron correlation in the PCM framework, we perform calculations on three symmetric ionized dimers

whose asymmetrically-charged, broken-symmetry ground states can be computed with MP theory (MP/PTE, MP/PTE-PTD, or MP/PTED schemes) and compared to ADC/SS-PCM and ADC/ptSS-PCM calculations of the formally identical charge-transfer state.

4.1.1 Cationic neon dimer. Ne_2^+ is the simplest system considered in this work. The ADC(2) gas-phase excitation energy or in other words the difference between the ground state and the FICT state is -0.77 eV. For the MP2 ground state of this simple, highly symmetrical system, IEF-PCM with $\epsilon = 32$ (typical of polar organic solvents) yields $\langle 0|\hat{R}(0)|0\rangle = 7.56$ eV for the solvation energy (note that this is not the solvation free energy, but just the solute-solvent interaction without the polarization work), regardless of whether the PTE, PTE-PTD, or PTED approach is employed.

For the respective FICT state, the ADC(2)/SS-PCM approach also yields a solvation energy of $\langle \text{CT}|\hat{R}(\text{CT})|\text{CT}\rangle = 7.56$ eV and, as evident from Fig. 2, the deviation of the solvent-relaxed total energies computed with the various approaches stays well below 0.5 meV along the whole scanned range of ϵ . This holds even for the non-iterative ptSS approach, which can be used to obtain a perturbative estimate of the energy of the solvent-relaxed state by using the value of the full dielectric constant ϵ also for the optical dielectric constant n^2 . This accuracy is surprising since perturbative, non-equilibrium corrections such as our ptSS correction⁹ or the "corrected linear response approach" of ref. 22 were designed to treat small density changes, whereas the FICT state involves a complete reversal of the 48 Debye dipole moment of $\text{Ne}^+ \cdots \text{Ne}$!

4.1.2 Cationic ethene dimer. For $(\text{C}_2\text{H}_4)_2^+$ the ADC(2)/cc-pVTZ gas-phase excitation energy is -0.34 eV. MP2/PTE with $\epsilon = 32$ affords a solvation energy of 6.05 eV and the PTE-PTD and PTED alternatives are almost identical at 6.04 eV. Differences between the total energies are even smaller and lie between 0.5 meV (PTE-PTED) and 5.0 meV (PTE-PTE-PTD); see Fig. 2.

Turning to the charge-inverted FICT state computed with ADC/SS-PCM, the solvation energy is just slightly larger at 6.11 eV. The difference between the total energies (Fig. 2), however, is much smaller. After correcting for the gas-phase excitation energy (*i.e.*, subtracting the difference between gas-phase MP ground-state and ADC excited-state energies), the differences between total energies obtained with ADC/SS-PCM remains below 2 meV compared to the MP/PTE and MP/PTED methods. Even the perturbative ptSS approach provides a reasonable estimate of the relaxed energy of the FICT state that lies within 50 meV of the self-consistent schemes.

4.1.3 Anionic nitromethane dimer. $(\text{CH}_3\text{NO}_2)_2^-$ is the largest and lowest-symmetry species of our three ionized dimers. In previous work on nitrobenzene,⁵⁵ it was established that the dipole moment and hence electrostatic nature of the nitro group differs significantly between the HF and MP description. The ADC(2)/cc-pVDZ gas-phase excitation energy of the FICT state is -0.66 eV. The MP2/PTE solute-solvent interaction energy is 7.08 eV for $\epsilon = 32$. The correlation-dependent electrostatics manifest in a significant lowering of the solvation energy to 6.75 eV, when the MP2/PTE-PTD scheme is employed, or 6.70 eV using MP2/PTED, and ADC(2)/SS-PCM affords a solvation energy of 6.75 eV for the FICT state. These pronounced differences relative to MP2/PTE originate from the impact of electron

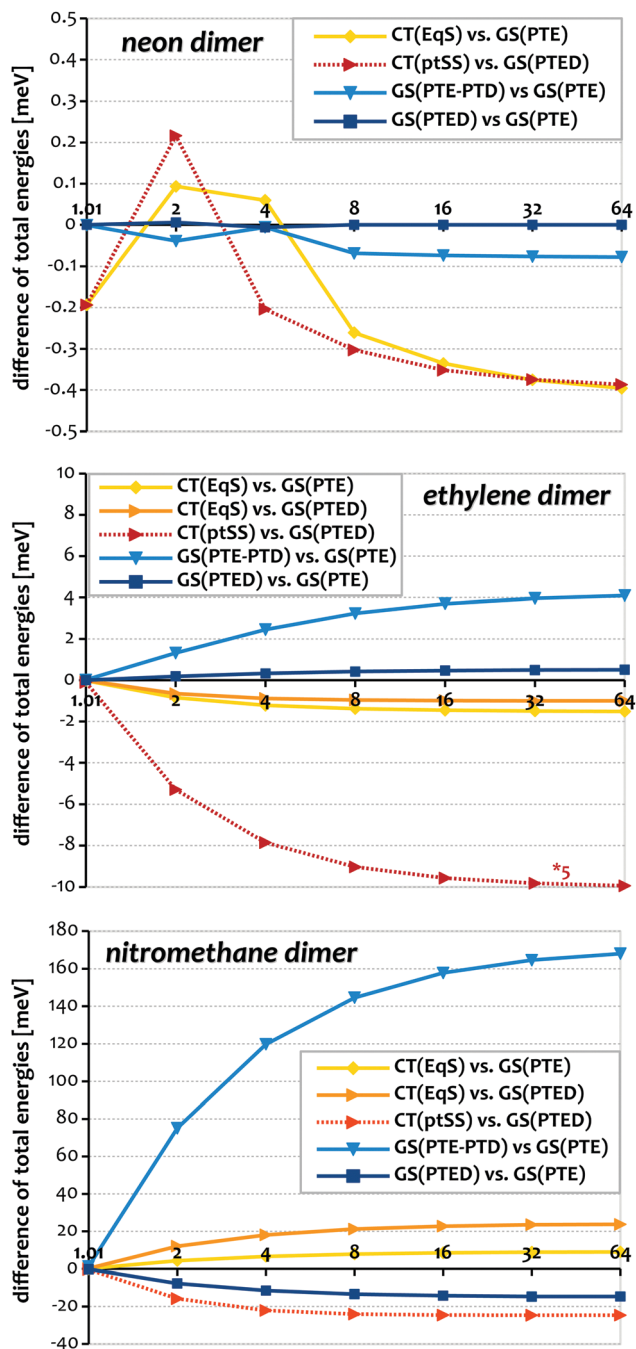


Fig. 2 Differences between the solvent-relaxed total energies of Ne_2^+ , $(\text{C}_2\text{H}_4)_2^+$, and $(\text{CH}_3\text{NO}_2)_2^-$, each with a separation of 1 nm between the monomers, computed using MP2/PTE, MP2/PTE-PTD, or MP2/PTED for the ground state and ADC(2)/SS-PCM equilibrium solvation (abbreviated EqS) or ADC(2)/ptSS for the formally identical charge-transfer (CT) state, as a function of ϵ (horizontal axis). For clarity, the difference between the gas-phase MP and ADC energies has been removed. The cc-pVTZ basis set is used for neon and ethene and the cc-pVDZ basis set for nitromethane.

correlation onto the dipole moment, which is 25% larger at the HF level than it is at the MP2 level. Despite these significant differences when correlation is included in the solvation energy, the total energies differ by less than 20 meV. The best agreement is obtained between the MP2/PTE and ADC(2)/SS-PCM approaches,

which afford a difference of 9 meV compared to 24 meV between MP2/PTED and ADC/SS-PCM. The PTE-PTD approach yields a total energy that differs from the other approaches by 140–200 meV.

4.1.4 Discussion. From these ionized dimer examples we see that solvent-relaxed total energies for symmetric, ionized dimers agree to within tens of meV across various methods, even in the case of $(\text{CH}_3\text{NO}_2)_2^-$ where correlation effects on the electrostatics are significant. For Ne_2^+ , where electron correlation is mostly irrelevant, the self-consistent and even the non-iterative ptSS approach afford essentially perfect agreement. We conclude that the description of excited-state solvation effects at the ADC(2)/SS-PCM level is essentially equivalent to the ground-state MP2/PTE and MP2/PTED methods, which validates the former.

Despite significant differences in the solvation energy predicted by the self-consistent PTE and PTED approaches for some of the cases, the resulting total energies agree with very high accuracy, consistent with the results of previous investigations.^{45–48} Consider the case of $(\text{CH}_3\text{NO}_2)_2^-$, for which the PTE and PTED total energies agree to within 20 meV across a broad range of dielectric constants, despite an electron correlation contribution of 380 meV. On the other hand, the PTE-PTD combination systematically deviates from the other approaches, despite the fact that its predicted solute–solvent interaction energies lie between those predicted by the PTE and PTED approaches.

Altogether, these findings strongly suggest that not only the PTED but also the PTE approach provides an adequate treatment of electron correlation effects in the solute–solvent interaction, whereas the correlation-corrected PTE-PTD approach appears to introduce a double-counting of these effects. Despite previous, successful applications in the framework of the non-equilibrium corrections within the ptSS approach for vertical excited states,⁹ the PTE-PTD correction cannot be recommended for the ground state.

4.2 Dimethylaminobenzonitrile

In this section the ADC(2)/SS-PCM and ADC(3)/SS-PCM methods are applied to investigate the photophysics of DMABN, a molecule that is perhaps the canonical example of “dual fluorescence” as a function of solvent polarity.⁵⁶ This feature originates in the presence of two low-lying excited states, one of which is a weakly dipole-allowed (the “locally excited” state, LE) and the other of which is characterized by intramolecular charge transfer (CT) that is strongly dipole allowed. While the former is the lowest excitation in gas phase and unpolar solution (*e.g.* cyclohexane), the CT state is supposed to become slightly lower in energy than LE in polar solution (*e.g.* acetonitrile), leading to a second fluorescence band ascribable to $S_2(\text{LE}) \rightarrow S_1(\text{CT})$ internal conversion. The details of the mechanism such as *e.g.* the involvement of an $\pi\sigma^*$ excited state and the interconversion between these states are, however, subject of an ongoing debate, which is beyond the scope of this work. For a recent overview, please be referred to ref. 57. Here, we merely employ DMABN to illustrate the accuracy of ADC/SS-PCM for the prediction of vertical fluorescence as well as relative state energies in solution. It has been reported that there exists a large discrepancy between

experimental and calculated fluorescence energies for the CT state of DMABN and related compounds in polar solvents.^{27,58} While the agreement for the LE and CT states in the gas phase and in non-polar solution is reasonable, the predicted ADC(2) fluorescence energies for the CT state of DMABN and related molecules are underestimated by more than 1 eV in polar solvents.^{27,58} This deviation is much larger than the typical ADC(2) error of 0.3–0.5 eV, and persists even when solvent effects on the excited-state structures are taken into account.²⁷

4.2.1 Computational approach. Ground and excited-state geometries have been computed in the gas phase at the RI-MP2/ and RI-ADC(2)/cc-pVDZ levels of theory, respectively. While for the ground and LE states only the fully relaxed structures are investigated, the relaxation of the CT state is explored in more detail. For this purpose, the relaxation is split into five intermediate steps beginning with a constrained, planar, CT-optimized structure (CT0), then twisting the amino group by 45 and 68 to 90° (CT45, CT68 and CT90), and eventually pyramidalizing the aromatic carbon (CT90P), as shown in Fig. 3. For each of these geometries, solvent-relaxed ground- and excited-state energies and properties as well as the non-equilibrium terms corresponding to vertical absorption or fluorescence were computed at the ADC(2)/SS-PCM/cc-pVDZ level of theory, with selected points treated at the ADC(3) level of theory. In all of these calculations, PCM parameters for cyclohexane ($\epsilon = 1.89$, $n^2 = 1.88$) or acetonitrile ($\epsilon = 36.7$, $n^2 = 1.81$) were used in combination with the IEF-PCM kernel.

Since the influence of the solvent is accounted for in a separate ADC/SS-PCM calculation for the fixed gas-phase geometries, this approach neglects the direct interaction of the geometric relaxation and solvation. In particular in case of the CT states, in which the solvent stabilization can be as large as 1 eV, there may be a significant influence onto the geometry. This might explain the larger discrepancies between the fluorescence energies computed for the CT state compared to those in the gas phase and non-polar solvents. An implementation of gradients for solvent-relaxed states computed with ADC/SS-PCM is in progress, but not yet available.

4.2.2 Results. MP2 and ADC(2) results are summarized in Fig. 3. Vertical excitation energies in the gas phase are 4.49 eV for the LE state (expt. = 4.13 eV) and 4.75 eV for the CT state (expt. = 4.57 eV). For acetonitrile solution, an ADC(2)/ptSS-PCM(PTED) calculation affords LE and CT states that are essentially degenerate at 4.39 eV. Calculated solvatochromatic shifts of -0.10 eV (LE) and -0.36 eV (CT) are in reasonable agreement with the experimental values, which are -0.27 eV and -0.34 eV, respectively. Excitation energies in cyclohexane lie between those computed for the gas phase and for acetonitrile. Experimental values for the cyclohexane-to-acetonitrile solvent shift in the LE state (-0.19 eV) and the CT state (-0.26 eV) are accurately reproduced at -0.14 eV and -0.25 eV, respectively.

On the horizontal axis of Fig. 3, we use a notation “X/Y” to indicate the state X on which the geometry is relaxed and the state Y to which the solvent is relaxed. For acetonitrile, full equilibration of the continuum solvent at the ground-state geometry (GS//LE or GS//CT) affords only a small energy reduction of 0.02 eV and 0.05 eV compared to the ptSS corrections of -0.05 eV (LE)

and -0.09 eV (CT). In cyclohexane, which does not possess a nuclear polarization component, the differences between ptSS-corrected non-equilibrium and solvent-relaxed energies are even smaller. In our experience, this is quite typical and even for polar solvents the ptSS corrections based on the electronic polarizability (reflected in n^2) often recover most of the energy reduction obtained with full relaxation of the solvent. This circumstance can be exploited to estimate the fully-relaxed energy of any state in a single calculation with the ptSS approach by setting the dielectric constant equal to n^2 .

Relaxation of the geometry of the solute for the LE state yields a much larger energy reduction than the solvent-field equilibration (*i.e.*, relaxation of the solvent geometry) and a slightly twisted structure with CCNC dihedral angle of 21°, 4.17 eV above the global ground-state minimum. This corresponds to a fluorescence energy of 3.73 eV that is very close to the experimental gas-phase value of 3.68 eV. The solvent-field equilibration for cyclohexane slightly reduces the energy of the LE state by only 0.06 eV, and the fluorescence energy predicted with the ptSS correction (3.65 eV) is quite close to the gas-phase value and is also in agreement with experimental data in hexane (3.65 eV).⁵⁹ The equilibrated solvent field of acetonitrile reduces the energy of the LE by 0.20 eV to 3.97 eV. At the same time, the energy of the ground state (in the non-equilibrium limit, *i.e.*, including ptSS terms) increases by 0.26 eV, to 0.70 eV. This yields a fluorescence energy of 3.26 eV, which agrees reasonably well with the experimental value of 3.44 eV.

Unconstrained relaxation of the geometry for the CT state in the gas phase yields a twisted and distorted structure (CCNC dihedral angle of 90°), in which the amino moiety is bent out of the aromatic plane. We label this structure CT90P, and it corresponds to ICT-D in ref. 27. The energy of the CT state for this structure is 3.91 eV, as compared to the twisted-only, C_{2v} -symmetric structure CT90 at 4.05 eV. Since the ground-state energy increases dramatically along the twisting and distortion coordinates, the calculated gas-phase fluorescence energy for CT90P is as low as 2.39 eV, far below the experimental value of 3.55 eV.

In non-polar cyclohexane, the CT state is stabilized by about 0.16 eV at the CT0 structure, 0.26 eV for CT90, and 0.11 eV for CT90P. As a result, the latter two structures are energetically much closer in non-polar solvents ($\Delta E = -0.04$ eV) than in gas phase ($\Delta E = -0.14$ eV). A much larger stabilization is seen in acetonitrile: 0.41 eV for CT0, then increasing to 0.73 eV along the twisting angle but reduced to 0.51 eV for the pyramidalized CT90P structure. This means that in acetonitrile the CT90 structure at 3.37 eV constitutes the minimum of the potential energy surface of the CT state, whereas CT90P is slightly (0.03 eV) higher in energy. This translates into a predicted fluorescence energy of merely 1.23 eV from the gas-phase minimum CT90P, much lower than the experimental value of 2.52 eV. Even if the energy minimum in solution (CT90) is taken as the origin of the fluorescence as suggested in ref. 27, the predicted energy is 1.83 eV and thus still much lower than the experimental value.

4.2.3 Discussion. We first discuss the disagreement between computed and measured fluorescence energy of the CT state of DMABN, which may be attributable to an overly static picture of

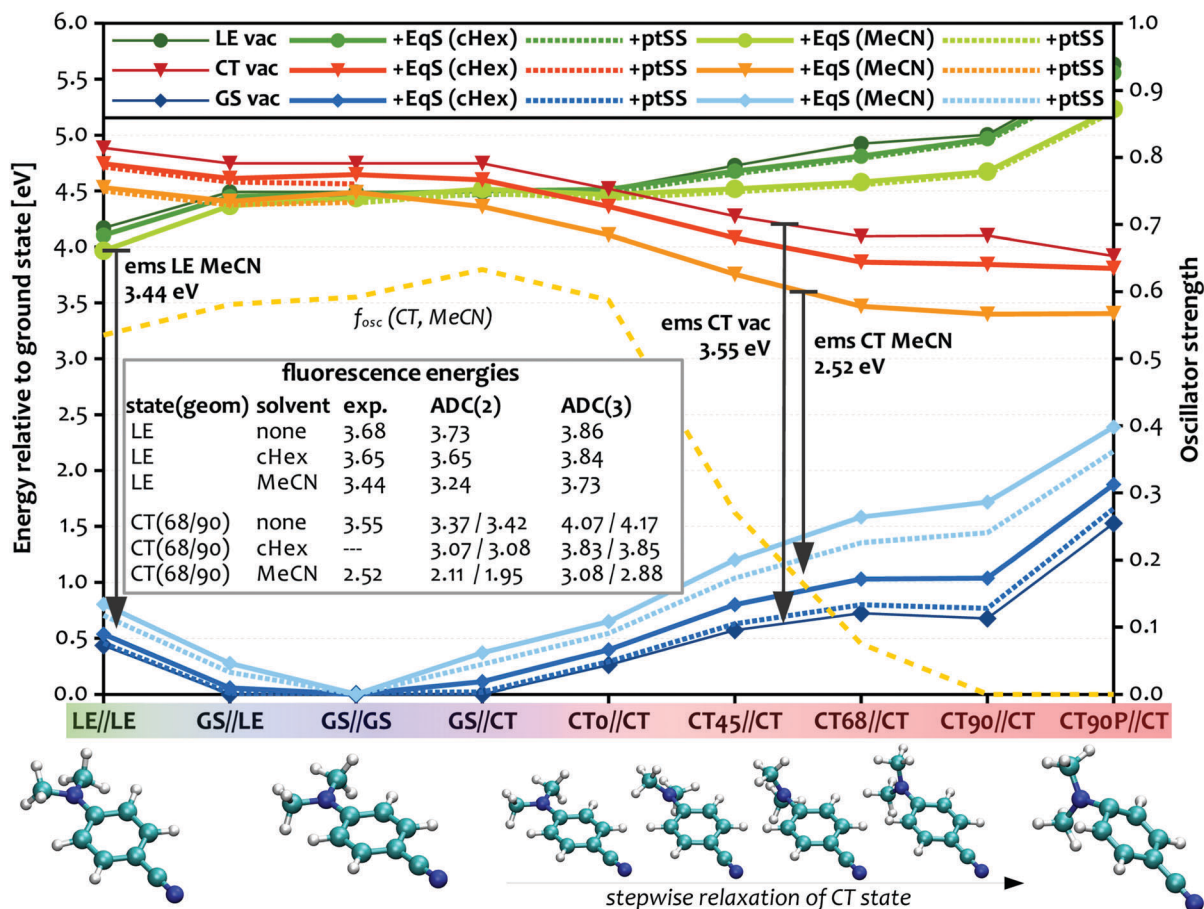


Fig. 3 Relative energies of the LE and CT states of DMABN for the ground state (GS) and excited-state (LE, CT0, CT45, CT68, CT90 and CT90P) optimized (all gas-phase) geometries without a solvent model (thin lines, dark colors), with equilibrium solvation (EqS) and PCM parameters for cyclohexane (bold lines, intermediate color), and EqS with parameters for acetonitrile (bold lines, bright color). All energies are given with respect to the energy of the ground-state in the respective solvent. Starting from the ground-state structure in the ground-state relaxed solvent field (GS//GS, blue), we use a notation "X//Y" as well as the color gradient on the x-axis to denote the subsequent relaxation of the geometry (X) and the solvent (Y), with respect to the LE state (to the left, green) and the CT state (to the right, red). Solid lines show the SS-PCM zeroth-order energies of the states in the frozen solvent-field of the reference state, while the dotted lines (only for non-reference, out-of-equilibrium states) show the first-order energy, which includes the ptSS non-equilibrium corrections (for a transition from the reference state). Selected experimental fluorescence energies are depicted as arrows and the remaining values (ref. 59) are given in the inset. The computed oscillator strength of the CT state (in acetonitrile solution) is plotted with respect to the secondary axis. All calculations were performed at the ADC(2)/SS-PCM/cc-pVDZ level of theory with IEF-PCM.

the fluorescence process. As usual, we have assumed that fluorescence occurs from the minimum of the excited-state potential surface and hence the maximum of the fluorescence spectrum is identified as the energy difference at the minimum-energy structure of the excited state. For the CT state of DMABN, however, the transition moment (f_{osc}) between the ground and CT state is exactly zero at the minimum (twisted intramolecular CT structures CT90 and CT90P), as evident from Fig. 3. As such, the maximum of the fluorescence spectrum most certainly does not originate from the twisted minimum-energy structure, but instead most of the fluorescence probably arises from less-twisted structures. For a reduction of the twisting angle to 68°, which costs about 0.18 eV in the gas phase (with respect to the CT90P minimum) and 0.10 eV in acetonitrile (with respect to CT90), f_{osc} increases to 0.1. Since the fluorescence energy strongly depends on the twisting angle in polar solvents (0.26 eV difference between CT90 and CT68 in CH₃CN) and

even more so on the distortion coordinate (0.72 eV between CT90P and CT90 in CH₃CN), a consideration of the twisting motion in combination with the actual minimum in solution significantly reduces the deviation between the computed and experimental values, to 0.41 eV or -0.20 eV assuming the maximum corresponds to CT68 or CT45, respectively. Turning this around, one can extrapolate that the twisting angle at which experimental and calculated values coincide lies between 50° and 55° (depicted as black arrows in Fig. 3). While the same argument applies to non-polar solvents as well, such solvents do not strongly modulate the excitation energy along the twisting coordinate (in particular between CT90 and CT68), which explains why the agreement is better already in the static picture in cyclohexane.

Turning to the switching of the dual fluorescence between polar and non-polar environments, we find that ADC(2) does not even provide a qualitatively correct picture. The computed

relative energies of the LE and CT states would not give rise to the observed behavior. Experimentally, emission is observed only from the LE state in gas phase and non-polar solvents, whereas in polar solvents there is strong emission from the CT state along with weak emission from the LE state. Assuming fast internal conversion between the two states, one would expect the CT state to lie far above the LE state (*i.e.*, CT thermally inaccessible) in the gas phase and non-polar solution, while in polar solution the relaxed minimum of the CT state should be situated slightly below the LE minimum (LE thermally accessible). At the ADC(2) level of theory, however, the relaxed minimum of the CT state lies slightly (0.05 eV) below that of the LE state already in the gas phase, and is 0.3 eV below the LE minimum in cyclohexane and 0.5 eV below in acetonitrile. We suspect that this arises from a deficiency for ADC(2), which in our experience overestimates the energetic impact of orbital relaxation and thus underestimates the energy of CT states relative to locally excited states. This is evident also from the predicted fluorescence energy, which agrees nicely for the LE state but is systematically underestimated for the CT state.

To examine how this changes at third order for perturbation theory, gas-phase and solvent-relaxed energies of the CT and LE states were recomputed at the ADC(3) level using ADC(2) geometries. We first carried out ADC(3) calculation in the solvent field relaxed with respect to the ADC(2) densities, and subsequently also in the fully consistent ADC(3) reaction field. As evident from Fig. 4, ADC(3) corrects the shortcomings of ADC(2) and already the difference between the vertical energies of the LE and CT states in the gas phase is about 0.2 eV larger. More importantly, the impact of the geometric relaxation of the CT state in the gas phase is reduced dramatically from 0.82 eV to 0.29 eV at the ADC(3) level of theory, while the influence of solvation is very similar. Altogether, ADC(3)/SS-PCM provides relative excited-state energies that are in excellent agreement with the experimentally observed behavior.

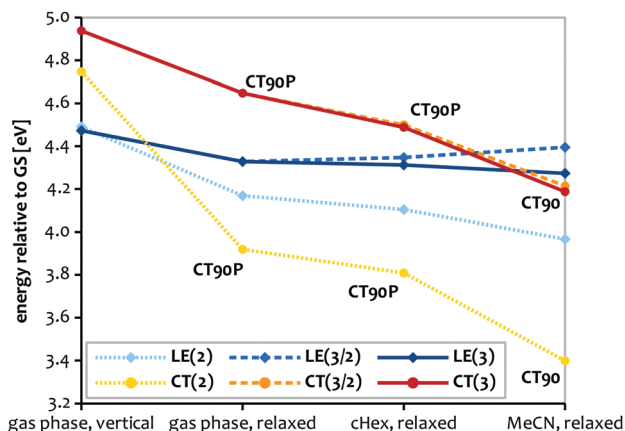


Fig. 4 Comparison of the vertical (gas-phase) and relaxed ADC/SS-PCM excitation energies of the LE (blue) and CT (orange) states of DMABN. Results are shown at both second order [ADC(2)] and third order, along with a mixed approach that uses ADC(3) with the ADC(2) reaction field. All calculations employ MP2/ADC(2) optimized gas-phase geometries.

Concerning the agreement between the mixed and consistent third-order approach for the solvent-field shown in Fig. 4, the differences are surprisingly largest for the LE state in acetonitrile, at 0.1 eV. This amounts to half of the total relaxation of the LE state in CH₃CN, and indicates that the mixed approach should be used with caution. One can, however, use the ptSS corrections of the reference state in the final ADC(3) calculation as a diagnostic tool. As long as they stay small (say, below 0.005 eV), the second- and third-order solute-solvent interactions are similar and the ADC(2) solvent field is appropriate. This is the case for the CT state, for which the ptSS terms are 0.004 eV and the difference between the approaches is only 0.02 eV. For the LE state, however, the ptSS terms amount to 0.02 eV, indicating a significant difference between the ADC(2) and ADC(3) solvent fields. In such a case, the fully consistent approach is advisable.

While ADC(3) certainly improves the relative energies of the CT and LE states compared to ADC(2), the agreement of the vertical fluorescence energies computed at this level of theory is slightly worse than with ADC(2). In our experience, this is typical for vertical excitation energies, which ADC(2) often overestimates as much as ADC(3) underestimates.⁶⁰ Consequently, the best estimate is usually the average of both methods, which appears to be the case here for fluorescence energies (see table in Fig. 3).

The results of our ADC(2)/SS-PCM approach qualitatively agree with the closely related ADC(2)/COSMO approach of Lunkenheimer *et al.*²⁷ Differences of up to 0.3 eV (but on average <0.1 eV) between ref. 27 and the present work are present in both the gas phase and in acetonitrile, and can be attributed to the use of slightly different geometries (ADC(2)/cc-pVDZ versus RI-CC2/TZVPP), basis sets (cc-pVDZ versus TZVPP), densities (ISR versus relaxed) van-der-Waals scaling factor used in construction of the solute cavity (1.3 versus 1.2) and the PCM itself (IEF-PCM versus COSMO). Adjusting all these parameters and using C-PCM rather than IEF-PCM, as it better resembles COSMO, we find both models agree to within 0.1 eV.

5 Summary and conclusions

It was demonstrated that a general, state-specific PCM in combination with an ADC(2) or ADC(3) description of the solute's electronic structure provides excellent energies of solvent-relaxed states and vertical transitions in solution. Since we limited our approach to the state-specific picture, where the solvent effect enters the quantum-chemical calculation only *via* one-electron charge-density Coulomb integrals, the underlying ADC equations are unmodified and the model can be used in combination with any flavor of ADC. Moreover, due to this clear separation between quantum-chemical part of the calculation and the solvent model, the results are presumably of general validity for both, the SS-PCM approach as well as the excited-state method.

To validate ADC/SS-PCM, a set of symmetric, ionized dimers was employed, whose lowest energy CT states are formally identical to the broken-symmetry ground state. Computing the latter using the well-established MP/PTE approach and comparing the results to the CT state computed using ADC/SS-PCM, the

deviation between the two methods was found to be <0.02 eV over a wide range of dielectric constants. This holds even for the challenging $(\text{CH}_3\text{NO}_2)_2^-$ case where electron correlation effects are large.

In addition to ADC/SS-PCM, we examined the “PTED” variant of the MP/PCM approach that introduces full self-consistency between the reaction field and the excited-state density, but found that differences with respect to the more affordable PTE approach were negligible. Hence, we conclude that even the PTE approach includes the impact of electron correlation on the total energy. Nevertheless, the uncorrelated PTE (SCF) solvent-field can be a source of errors, e.g. in the calculation of vertical excitation energies. For this reason, we introduced the PTE-PTD (formerly PTD) approach, which was successfully applied to improve computed excitation energies in the non-equilibrium formalism in ref. 9. Applied to the ground state, however, large deviations from the other approaches were encountered for this *a posteriori* correlation correction. This was traced back to a double-counting of correlation effects, and we thus discourage the use of the respective correlation correction for the ground state.

Ultimately, ADC/SS-PCM was employed to investigate solvent-relaxed potential energy surfaces of 4-(*N,N*)-dimethylamino-benzonitrile (DMABN). The agreement with experimental fluorescence data is excellent for the LE state under all circumstances, in particular with ADC(2). For the CT state, however, it was demonstrated that an intra-molecular twisting coordinate has to be considered in detail to achieve a similar agreement. In general, the agreement of ADC(2)/SS-PCM is consistently better than for ADC(3) for fluorescence energies. For the relative energies of the LE and CT states, however, only ADC(3) yields results that are consistent with the experimental observation of dual fluorescence in polar solvents but not in non-polar ones. This was traced back to an underestimation of the energy of the CT state compared to the LE state at second order of perturbation theory.

After all, the ADC/SS-PCM approach constitutes valuable tool that enables an accurate yet efficient description of solvent-relaxed excited states and transitions in solution at up to third order of ADC.

Acknowledgements

John M. Herbert acknowledges funding from the Alexander von Humboldt Foundation. Jan-Michael Mewes wants to thank the Interdisciplinary Center for Scientific Computing for funding and computer time and acknowledges funding from the Alexander von Humboldt foundation.

References

- J. Tomasi, B. Mennucci and R. Cammi, *Chem. Rev.*, 2005, **105**, 2999–3093.
- R. A. Friesner and V. Guallar, *Annu. Rev. Phys. Chem.*, 2005, **56**, 389–427.
- H. M. Senn and W. Thiel, *Angew. Chem., Int. Ed. Engl.*, 2009, **48**, 1198–1229.
- D. G. Fedorov and K. Kitaura, *J. Phys. Chem. A*, 2007, **111**, 6904–6914.
- M. S. Gordon, D. G. Fedorov, S. R. Pruitt and L. V. Slipchenko, *Chem. Rev.*, 2012, **112**, 632–672.
- M. W. van der Kamp and A. J. Mulholland, *Biochemistry*, 2013, **52**, 2708–2728.
- L. D. Jacobson, R. M. Richard, K. U. Lao and J. M. Herbert, *Annu. Rep. Comput. Chem.*, 2013, **9**, 25–56.
- K. U. Lao and J. M. Herbert, *J. Phys. Chem. A*, 2015, **119**, 235–252.
- J.-M. Mewes, Z.-Q. You, M. Wormit, T. Kriesche, J. M. Herbert and A. Dreuw, *J. Phys. Chem. A*, 2015, **119**, 5446–5464.
- A. A. J. Aquino, I. Borges, R. Nieman, A. Kohn and H. Lischka, *Phys. Chem. Chem. Phys.*, 2014, **16**, 20586–20597.
- Š. Budzák, P. Mach, M. Medved' and O. Kysel', *Phys. Chem. Chem. Phys.*, 2015, **17**, 17618–17627.
- S. Yomosa, *J. Phys. Soc. Jpn.*, 1974, **36**, 1655–1660.
- R. Bonaccorsi, R. Cimraglia and J. Tomasi, *J. Comput. Chem.*, 1983, **4**, 567–577.
- H. J. Kim and J. T. Hynes, *J. Chem. Phys.*, 1990, **93**, 5194–5210.
- A. Klamt, *J. Phys. Chem.*, 1996, **100**, 3349–3353.
- B. Mennucci, R. Cammi and J. Tomasi, *J. Chem. Phys.*, 1998, **109**, 2798–2807.
- R. Cammi and J. Tomasi, *Int. J. Quantum Chem., Symp.*, 1995, **29**, 465–474.
- M. Cossi and V. Barone, *J. Phys. Chem. A*, 2000, **104**, 10614–10622.
- R. Improta, V. Barone, G. Scalmani and M. J. Frisch, *J. Chem. Phys.*, 2006, **125**, 054103.
- A. Dreuw and M. Wormit, *Wiley Interdiscip. Rev.: Comput. Mol. Sci.*, 2015, **5**, 82–95.
- Z.-Q. You, J.-M. Mewes, A. Dreuw and J. M. Herbert, *J. Chem. Phys.*, 2015, **143**, 204104.
- M. Caricato, B. Mennucci, J. Tomasi, F. Ingrosso, R. Cammi, S. Corni and G. Scalmani, *J. Chem. Phys.*, 2006, **124**, 124520.
- M. Caricato, *J. Chem. Theory Comput.*, 2012, **8**, 5081–5091.
- M. Caricato, *J. Chem. Phys.*, 2013, **139**, 044116.
- M. Caricato, *Comput. Theor. Chem.*, 2014, **1040**, 99–105.
- A. Klamt and G. Schüürmann, *J. Chem. Soc., Perkin Trans. 2*, 1993, 799–805.
- B. Lunkenheimer and A. Köhn, *J. Chem. Theory Comput.*, 2013, **9**, 977–994.
- R. Cammi and B. Mennucci, *J. Chem. Phys.*, 1999, **110**, 9877–9886.
- M. Cossi and V. Barone, *J. Chem. Phys.*, 2001, **115**, 4708–4717.
- V. Barone and M. Cossi, *J. Phys. Chem. A*, 1998, **102**, 1995–2001.
- J. Liu and W. Liang, *J. Chem. Phys.*, 2013, **138**, 024101.
- R. Cammi, S. Corni, B. Mennucci and J. Tomasi, *J. Chem. Phys.*, 2005, **122**, 104513.
- R. Improta, G. Scalmani, M. J. Frisch and V. Barone, *J. Chem. Phys.*, 2007, **127**, 74504.
- J. Wenzel, M. Wormit and A. Dreuw, *J. Comput. Chem.*, 2014, **35**, 1900–1915.
- J. Wenzel, A. Holzer, M. Wormit and A. Dreuw, *J. Chem. Phys.*, 2015, **142**, 214104.
- C. M. Krauter, M. Pernpointner and A. Dreuw, *J. Chem. Phys.*, 2013, **138**, 044107.

- 37 D. Lefrancois, M. Wormit and A. Dreuw, *J. Chem. Phys.*, 2015, **143**, 124107.
- 38 F. Plasser, B. Thomitzni, S. A. Bäßler, J. Wenzel, D. R. Rehn, M. Wormit and A. Dreuw, *J. Comput. Chem.*, 2015, **36**, 1609–1620.
- 39 A. W. Lange and J. M. Herbert, *J. Chem. Phys.*, 2010, **133**, 244111.
- 40 E. Cancés, B. Mennucci and J. Tomasi, *J. Chem. Phys.*, 1997, **107**, 3032–3041.
- 41 D. M. Chipman, *J. Chem. Phys.*, 1997, **106**, 10194–10206.
- 42 D. M. Chipman, *J. Chem. Phys.*, 2000, **112**, 5558–5565.
- 43 C. J. F. Bottcher, O. V. Belle, P. Bordewijk and A. Rip, *Theory of Electric Polarization*, Elsevier, 1973, vol. 1.
- 44 J. Tomasi and M. Persico, *Chem. Rev.*, 1994, **94**, 2027–2094.
- 45 J. Ángyán, *Chem. Phys. Lett.*, 1995, **241**, 51–56.
- 46 F. J. Olivares del Valle and J. Tomasi, *Chem. Phys.*, 1991, **150**, 139–150.
- 47 M. A. Aguilar, F. J. Olivares del Valle and J. Tomasi, *Chem. Phys.*, 1991, **150**, 151–161.
- 48 F. J. Olivares del Valle, R. Bonaccorsi, R. Cammi and J. Tomasi, *THEOCHEM*, 1991, **230**, 295–312.
- 49 Y. Shao, Z. Gan, E. Epifanovsky, A. T. B. Gilbert, M. Wormit, J. Kussmann, A. W. Lange, A. Behn, J. Deng, X. Feng, D. Ghosh, M. Goldey, P. R. Horn, L. D. Jacobson, I. Kaliman, R. Z. Khaliullin, T. Kús, A. Landau, J. Liu, E. I. Proynov, Y. M. Rhee, R. M. Richard, M. A. Rohrdanz, R. P. Steele, E. J. Sundstrom, H. L. Woodcock III, P. M. Zimmerman, D. Zuev, B. Albrecht, E. Alguire, B. Austin, G. J. O. Beran, Y. A. Bernard, E. Berquist, K. Brandhorst, K. B. Bravaya, S. T. Brown, D. Casanova, C.-M. Chang, Y. Chen, S. H. Chien, K. D. Closser, D. L. Crittenden, M. Diedenhofen, R. A. DiStasio Jr., H. Dop, A. D. Dutou, R. G. Edgar, S. Fatehi, L. Fusti-Molnar, A. Ghysels, A. Golubeva-Zadorozhnaya, J. Gomes, M. W. D. Hanson-Heine, P. H. P. Harbach, A. W. Hauser, E. G. Hohenstein, Z. C. Holden, T.-C. Jagau, H. Ji, B. Kaduk, K. Khistyayev, J. Kim, J. Kim, R. A. King, P. Klunzinger, D. Kosenkov, T. Kowalczyk, C. M. Krauter, K. U. Lao, A. Laurent, K. V. Lawler, S. V. Levchenko, C. Y. Lin, F. Liu, E. Livshits, R. C. Lochan, A. Luenser, P. Manohar, S. F. Manzer, S.-P. Mao, N. Mardirossian, A. V. Marenich, S. A. Maurer, N. J. Mayhall, C. M. Oana, R. Olivares-Amaya, D. P. O'Neill, J. A. Parkhill, T. M. Perrine, R. Peverati, P. A. Pieniazek, A. Prociuk, D. R. Rehn, E. Rosta, N. J. Russ, N. Sergueev, S. M. Sharada, S. Sharma, D. W. Small, A. Sodt, T. Stein, D. Stück, Y.-C. Su, A. J. W. Thom, T. Tsuchimochi, L. Vogt, O. Vydrov, T. Wang, M. A. Watson, J. Wenzel, A. White, C. F. Williams, V. Vanovschi, S. Yeganeh, S. R. Yost, Z.-Q. You, I. Y. Zhang, X. Zhang, Y. Zhou, B. R. Brooks, G. K. L. Chan, D. M. Chipman, C. J. Cramer, W. A. Goddard III, M. S. Gordon, W. J. Hehre, A. Klamt, H. F. Schaefer III, M. W. Schmidt, C. D. Sherrill, D. G. Truhlar, A. Warshel, X. Xue, A. Aspuru-Guzik, R. Baer, A. T. Bell, N. A. Besley, J.-D. Chai, A. Dreuw, B. D. Dunietz, T. R. Furlani, S. R. Gwaltney, C.-P. Hsu, Y. Jung, J. Kong, D. S. Lambrecht, W. Liang, C. Ochsenfeld, V. A. Rassolov, L. V. Slipchenko, J. E. Subotnik, T. Van Voorhis, J. M. Herbert, A. I. Krylov, P. M. W. Gill and M. Head-Gordon, *Mol. Phys.*, 2014, 184–215.
- 50 T. H. Dunning, Jr., *J. Chem. Phys.*, 1989, **90**, 1007–1023.
- 51 A. Bondi, *J. Phys. Chem.*, 1964, **68**, 441–451.
- 52 R. S. Rowland and R. Taylor, *J. Phys. Chem.*, 1996, **100**, 7384–7391.
- 53 F. Neese, *Wiley Interdiscip. Rev.: Comput. Mol. Sci.*, 2012, **2**, 73–78.
- 54 R. Ahlrichs, M. Bär, M. Häser, H. Horn and C. Kölmel, *Chem. Phys. Lett.*, 1989, **162**, 165–169.
- 55 J.-M. Mewes, V. Jovanovic, C. M. Marian and A. Dreuw, *Phys. Chem. Chem. Phys.*, 2014, **16**, 12393–12406.
- 56 Z. R. Grabowski, K. Rotkiewicz and W. Rettig, *Chem. Rev.*, 2003, **103**, 3899–4032.
- 57 I. Georgieva, A. J. A. Aquino, F. Plasser, N. Trendafilova, A. Köhn and H. Lischka, *J. Phys. Chem. A*, 2015, **119**, 6232–6243.
- 58 M. V. Bohnwagner, I. Burghardt and A. Dreuw, *J. Phys. Chem. A*, 2016, **120**, 14–27.
- 59 S. I. Druzhinin, N. P. Ernstring, S. A. Kovalenko, L. P. Lustres, T. A. Senyushkina and K. A. Zachariasse, *J. Phys. Chem. A*, 2006, **110**, 2955–2969.
- 60 P. Harbach, M. Wormit and A. Dreuw, *J. Chem. Phys.*, 2014, **141**, 064113.